Supply Shocks and Inflationary Pressures in Global Value Chains: The Role of Network Centrality*

Yojiro Ito Harumasa Shirakawa

Abstract

We examine supply shock propagation through global value chains. To capture network heterogeneity, we construct a 30,000-node international input-output table by disaggregating sectoral data using product-level trade microdata. Integrating this with an identification of supply shocks leveraging micro-level quantity fluctuations, we find that high network centrality dampens price pass-through by 40%. In contrast, while centrality typically amplifies quantity adjustments, this mechanism vanished during the COVID-19 recovery, suggesting that physical bottlenecks restricted substitution pathways. These findings suggest that price stability at the network core masks accumulating physical shortages, creating latent risks of non-linear inflationary surges as supply constraints eventually bind.

Keywords: Global Value Chains, Supply Shocks, Network Centrality, Inflation
JEL Classification: E31, F14, F41, D57, L14

*First version: July 2025. This version: January 2026. Preliminary and incomplete. Comments are welcome. The authors would like to thank Diego Comin for his helpful suggestions during the initial stages of this research, and Mototsugu Shintani for his valuable comments. We also thank staff at the Bank of Japan for their insightful discussions and feedback. The views expressed in this paper are those of the authors and do not necessarily reflect the official views of the Bank of Japan. Ito: Institute for Monetary and Economic Studies, Bank of Japan (Email: youjirou.itou@boj.or.jp). Shirakawa: Institute for Monetary and Economic Studies, Bank of Japan (Email: harumasa.shirakawa@boj.or.jp).

1 Introduction

The global inflationary episode in the aftermath of the COVID-19 pandemic has fundamentally reshaped our understanding of macroeconomic stability, highlighting the profound impact of supply chain disruptions. As production processes have become increasingly fragmented across national borders, Global Value Chains (GVCs) have evolved from mere conduits of trade into complex filters of global shocks. While recent literature has extensively documented the role of GVCs in transmitting shocks, we still lack a micro-founded understanding of how the network's structural topology modulates price and quantity adjustments. Crucially, the mechanism through which specific network nodes can either amplify or dampen inflationary signals remains a "black box" in contemporary macroeconomics.

A primary obstacle to understanding these mechanisms has been the dual limitation of existing data resolution and identification universality. First, standard international input-output (ICIO) tables, such as the OECD ICIO, rely on aggregate sectors that mask critical heterogeneity. As Antras et al. (2012) highlight, such coarse classifications prevent researchers from identifying specific "micro-bottlenecks"—systemically pervasive intermediate goods (Jones, 2011; Barrot and Sauvagnat, 2016) like semiconductors that function as the infrastructure of global production. Second, even when high-resolution data are available, the causal identification of shocks has remained restricted to specific empirical domains. While a growing literature has adopted empirical designs based on high-dimensional fixed-effects (HDFE) or leave-one-out (LOO) strategies to isolate exogenous shocks, their application has remained largely domain-specific. Prominent examples include the analysis of firm-level price pass-through within a single economy (Amiti, Itskhoki, and Konings, 2019) or the industry-level propagation of final demand shocks (Ferrari, 2025). This absence of a universal, supply-side identification framework applicable across the entire spectrum of traded goods has prevented a systematic mapping of idiosyncratic production disruptions onto the global network.

We address these fundamental challenges by developing an empirical framework that integrates high-resolution trade microdata with a comprehensive identification engine. First, we construct a "high-granularity ICIO table" by systematically disaggregating standard ICIO structures along both the supply and use dimensions: we refine the supply side (rows) using bilateral trade flows at the Harmonized System (HS) 6-digit level and the use side (columns) by applying detailed industry production recipes. This procedure results in a massive global production matrix spanning 76 countries and 388 sectors with over 218 million linkages, enabling us to uncover "shadow hubs" that possess immense structural centrality despite modest trade values. Second, we generalize the logic of HDFE and LOO strategies into a universal, supply-side identification framework. Crucially, while existing frontier studies such as Ferrari (2025) identify shocks using industry-level trade values, we extend this methodology to the supply side by utilizing physical quantities across more than 5,000 product categories. By extracting idiosyncratic exporter-specific shifters from quantities rather than values, we provide

a consistent measure of supply shocks that is fundamentally decoupled from price fluctuations and destination-specific demand. This methodological advancement effectively transforms the theoretical concept of network propagation into a measurable empirical parameter, providing a general-purpose research design for analyzing shock transmission in global production networks.

Leveraging this framework, we document two distinct empirical regularities in shock propagation. First, we identify a persistent "structural buffer effect" in price formation: products with high structural centrality exhibit significantly dampened price increases in response to negative supply shocks. Quantitatively, for a product with centrality one standard deviation above the average, the price hike is mitigated by approximately 40% relative to the baseline. Second, we uncover a profound regime shift in quantity adjustment dynamics. While network centrality typically amplifies adjustments through a "chain of substitution" in standard economic environments, this mechanism was effectively paralyzed during the COVID-19 recovery period. We term this phenomenon "topological neutralization," as the network-driven amplification vanished even while importers' fundamental price sensitivity remained stable.

These findings provide empirical validation for the theoretical tension between price rigidities and network-driven substitution. The structural buffering we observe aligns with the logic of Pasten, Schoenle, and Weber (2020), who demonstrate that central nodes characterized by price rigidities—or "sticky hubs"—can function as structural anchors for the aggregate price level. The pivotal role of these nodes may incentivize firms to maintain price stability through long-term relational contracts to safeguard future trade rents (Macchiavello, 2022), providing a micro-founded rationale for this structural stickiness. Conversely, the collapse of quantity amplification during the pandemic recovery provides empirical support for the non-linear propagation models of Baqaee and Farhi (2019, 2022). In their framework, the network's capacity to dissipate shocks hinges on the elasticity of substitution; when physical bottlenecks compromise this ease of substitution, the network ceases to act as a stabilizer. Our results suggest that "topological neutralization" is a manifest case of this theoretical nonlinearity, where supply-side constraints effectively choked off the substitution pathways typically afforded by central nodes.

These findings offer significant implications for the monitoring of global inflationary pressures. The persistent price-buffering role of structural anchors implies a potential "signal attenuation" where inflationary pressures remain latent in official indices even as physical disruptions accumulate. This structural decoupling suggests that price stability at the network's core can act as a veil, masking the accumulation of physical shortages—a scenario that mirrors the classic trade-off between price and quantity signals discussed by Weitzman (1974) and the literature on shadow prices (Bhattacharyya et al., 2019). By uncovering these latent dynamics, our framework provides a structural indicator to identify these hidden bottlenecks and assess the resilience of the global production network from a topological perspective.

Related Literature. Our work contributes to three strands of literature. First, we provide a large-scale empirical bridge to the theoretical literature on the network origins of macroeconomic

fluctuations and granularity (Gabaix, 2011; Acemoglu et al., 2012; Carvalho, 2014; Baqaee and Farhi, 2019). While foundational studies establish how idiosyncratic shocks can aggregate into systemic volatility, their quantitative applications have been largely constrained by a reliance on standard, relatively coarse industry classifications. By scaling the network analysis to over 30,000 nodes, we offer a high-resolution empirical validation that uncovers "shadow hubs" and non-linearities that remain invisible at higher levels of aggregation.

Second, we add to the empirical literature identifying supply-side shocks through trade microdata (e.g., Hummels et al., 2014; Amiti, Itskhoki, and Konings, 2019; Ferrari, 2025). Unlike existing studies that are frequently restricted to single-country settings or specific event-studies, our framework implements a universal identification strategy across a global HS 6-digit panel. By extracting idiosyncratic exporter-specific shifters from physical quantities rather than values, we ensure our identified shocks are fundamentally decoupled from price fluctuations and destination-specific demand, providing a general-purpose research design applicable to the entire spectrum of traded goods.

Third, we contribute to the growing body of research on GVC dynamics during the COVID-19 pandemic and its inflationary consequences (e.g., Carvalho et al., 2021; di Giovanni et al., 2022; Santacreu and LaBelle, 2022). While these studies have successfully quantified the transmission of aggregate shocks, the specific mechanism through which network topology filters or masks price signals remains relatively under-explored. We extend this line of inquiry by uncovering "topological neutralization"—the collapse of substitution pathways under systemic pressure—and documenting the resulting "signal attenuation." By providing a structural explanation for why inflationary pressures may remain latent despite severe physical disruptions, we offer a micro-founded bridge between the network theories of price-setting (Pasten, Schoenle, and Weber, 2020) and the practical challenges of post-pandemic inflation monitoring.

The remainder of the paper is organized as follows. Section 2 describes the empirical framework and the identification strategy. Section 3 presents the structural properties of the GVC, followed by the empirical results on price responses and quantity adjustments. Section 4 concludes.

2 Empirical Framework

To investigate the propagation of supply shocks through global value chains (GVCs), we develop a multi-step empirical framework. We first describe the data sources and the construction of our high-granularity international input-output (ICIO) table. We then detail our identification strategy for isolating idiosyncratic supply shocks and our empirical specification for estimating trade elasticities.

2.1 Data Sources

Our analysis integrates three primary datasets, each serving a distinct role in our empirical framework.

First, we utilize the OECD Inter-Country Input-Output (ICIO) tables (2023 edition) as our global accounting backbone.[1] The dataset covers 76 economies and 45 aggregate sectors from 1995 to 2020. Second, we employ the CEPII BACI database, which provides bilateral trade flows at the Harmonized System (HS) 6-digit level (covering approximately 5,000 product categories) for the period 1995–2023. Third, we use the U.S. Bureau of Economic Analysis (BEA) Detailed Input-Output tables (2007, 2012, and 2017 benchmark years), which identify approximately 400 industries, as our reference technology.

Crucially, these datasets are utilized at different stages of our analysis. The high-granularity ICIO table, which serves as the basis for calculating network metrics such as centrality, is constructed by merging all three datasets (OECD ICIO, BACI, and BEA). In contrast, the idiosyncratic supply shifters described in Section 2.4 are estimated exclusively using the raw bilateral trade microdata from the BACI database. This distinction ensures that our identified supply shocks are derived directly from observed trade fluctuations, independent of any assumptions made during the ICIO disaggregation process.

2.2 A High-Granularity ICIO

To overcome the aggregation bias inherent in standard ICIO tables, we construct a "high-granularity ICIO" through a hybrid approach. This process disaggregates the broad sector-to-sector flows into product-to-industry transactions.

Formally, let i and j denote the exporter and importer countries, respectively. Let R and S denote the aggregate sectors in the ICIO, and let r and s denote the granular sub-sectors (products or industries) such that $r \in R$ and $s \in S$. We estimate the flow x_{ij}^{rs} from sub-sector r in country i to sub-sector s in country j as follows:

$$x_{ij}^{rs} = \left(\sum_{S} Z_{ij}^{RS} \right) \times \alpha_{ij}^{r} \times \beta_{r \to s} \tag{1}$$

where $\sum_S Z_{ij}^{RS}$ represents the total value of intermediate exports from sector R in country i to all industries in country j, extracted from the OECD ICIO. The term $\beta_{r \to s}$ is the technical allocation coefficient representing the share of product r used as an intermediate input by industry s, derived from the BEA Detailed Input-Output tables.

[1] We choose the OECD ICIO tables over the World Input-Output Table (WIOT) from the World Input-Output Database (WIOD), provided by the Groningen Growth and Development Centre at the University of Groningen, primarily due to their extended temporal coverage. While the latest WIOT (2016 release) only provides data up to 2014, the OECD ICIO covers the period up to 2020. This allows us to align our analysis with the full sample period of the trade data and to capture the structural shifts induced by the COVID-19 pandemic.

The allocation share α_{ij}^{r} captures the composition of sub-sector r within the aggregate sector R. For tradable sectors, α_{ij}^{r} is calculated as the bilateral trade share from the CEPII BACI database.[2] For non-tradable sectors and domestic transactions (where $i = j$), where product-level trade data are unavailable, we utilize the internal industry shares from the BEA tables to disaggregate the ICIO flows. While this assumes that the domestic industry composition mirrors that of the U.S., we expect this approximation to have a negligible impact on our findings, as GVC centrality and international inflation propagation are predominantly driven by cross-border trade in intermediate goods.

Following the "reference technology" assumption widely adopted in the trade literature (e.g., Nunn, 2007; Antràs and Chor, 2018), we assume that the detailed input requirements observed in the U.S. serve as a valid proxy for the technical coefficients of corresponding industries in other economies.

To align these coefficients with the temporal scope of our trade data (1995–2023), we utilize the BEA benchmark years (2007, 2012, and 2017) and apply linear interpolation for intermediate years, supplemented by constant back-filling for the pre-2007 period and forward-filling for the post-2017 period. Similarly, for the OECD ICIO tables, we assume that the structural linkages remain constant beyond 2020 and forward-fill the 2020 structure to cover the remaining years of our sample (2021–2023).

This construction procedure results in a massive global production network that significantly expands the resolution of existing ICIO tables. Specifically, our high-granularity ICIO covers 76 countries and 388 sectors, yielding approximately 30,000 unique country-sector nodes. By disaggregating the data to this level, we identify over 218 million potential international and domestic linkages. This high-resolution structure enables us to uncover the aforementioned "shadow hubs" and capture non-linear propagation effects that remain invisible at higher levels of aggregation.

2.3 Measuring GVC Centrality

To quantify the structural importance of each node within the global production network, we compute a measure of network centrality for each country-industry pair. The starting point for our centrality measure is the economic intuition that the structural importance of a supplier is endogenously determined by the importance of its customers. In a production network, a sector is considered central if it provides essential inputs to other highly central sectors, thereby acting as a critical hub for downstream value creation.

This recursive logic—where a node's influence is the sum of the influences of the nodes it supplies—is a hallmark of multisector models with input-output linkages, most notably formalized by Acemoglu et al. (2012). We define the centrality vector v as satisfying the

[2] A potential concern is that bilateral trade flows include both intermediate and final goods. In future iterations of this paper, we plan to refine this decomposition by excluding product categories primarily classified as final consumption goods to further isolate pure intermediate linkages.

following structural relationship:

$$v' = f' + \alpha v' W \tag{2}$$

where f is a vector representing the initial external impulse originating from each node, and W is the $N \times N$ global direct requirement matrix derived from our high-granularity ICIO. The parameter $\alpha \in (0, 1)$ serves as a decay factor reflecting the weight of intermediate linkages. By solving for v, we obtain:

$$v' = f'(I - \alpha W)^{-1} \tag{3}$$

where $(I - \alpha W)^{-1}$ is the global Leontief inverse matrix.

Expanding this relationship into an infinite series provides the economic intuition:

$$v' = f' + \alpha f' W + \alpha^2 f' W^2 + \alpha^3 f' W^3 + \dots \tag{4}$$

The first term, f', represents the direct impact of a supply-side impulse. The subsequent terms, $\alpha^n f' W^n$, capture the n-th order cascades as the shock ripples through downstream sectors and across national borders. A high centrality score indicates that a shock to a specific node has a large cumulative impact on the global economy through the entire infinite chain of subsequent production stages.

To isolate the pure structural centrality, we assume a uniform demand distribution by setting $f = \frac{1}{N}\mathbf{1}$. This ensures our metric is mathematically equivalent to Katz Centrality (Katz, 1953) and Forward Linkages Miller and Blair (2022). This formulation allows our measure to be interpreted as the principal eigenvector of the production network under a non-homogeneous impulse, identifying the stationary distribution of structural influence.

Due to the high dimensionality of our ICIO matrix, directly computing the Leontief inverse $(I - \alpha W)^{-1}$ is computationally prohibitive. In practice, we approximate v by iteratively summing the power series in Eq. (4) until the centrality scores converge, ensuring that we capture the full depth of the global value chain. By identifying nodes with the highest values in v, we structurally locate what we term *Shadow Hubs*: sectors that function as critical systemic conduits despite their modest trade volumes. In our baseline specification, we set $\alpha = 0.5$, consistent with the average share of intermediate inputs observed in our dataset.

2.4 Identification: Supply Shifters

The central empirical challenge in estimating trade elasticities is the simultaneity of supply and demand shocks. To address this, we isolate idiosyncratic supply-side fluctuations at the exporter-product level using a high-dimensional fixed-effects approach. This strategy allows us to extract a universal shifter applicable to all trade flows, overcoming the limitations of "intermittent" instruments such as tariff changes that are often restricted to specific products or time periods.

We construct our supply shifter, $\hat{\eta}_{i,k,t}^{(-j)}$, for each exporter i, product k, and year t, utilizing the

rich variation in bilateral trade microdata from the CEPII BACI database. Our identification strategy builds on the "leave-one-out" (LOO) logic that has become a standard practice in the international trade and labor literature to isolate idiosyncratic shocks (e.g., Autor et al., 2013; Hummels et al., 2014). Specifically, we follow the spirit of Amiti et al. (2019) and Ferrari (2025) in using high-dimensional fixed effects to capture exporter-specific shifts that are exogenous to a given destination. While the fundamental logic of using rest-of-the-world fluctuations is well-established, we introduce a critical refinement by extracting these shifters from a panel of export *quantities* ($\ln q$) rather than values. This distinction is vital: by relying on physical volumes, we ensure that the identified shifter reflects genuine shifts in production capacity and idiosyncratic productivity shocks, avoiding the mechanical contamination from price fluctuations that often plagues value-based instruments.

Formally, for each target importer j, we identify the exporter-specific supply shock by estimating a fixed-effects model on the panel of all bilateral trade flows excluding those directed to country j. Let $\mathcal{J}$ be the set of all countries in our sample. For a given target $j \in \mathcal{J}$, we estimate the following specification:

$$\Delta \ln q_{i,n,k,t} = \eta_{i,k,t}^{(-j)} + FE_{n,t} + \epsilon_{i,n,k,t}, \quad \forall n \in \mathcal{J} \setminus \{j\} \tag{5}$$

where $q_{i,n,k,t}$ is the import quantity of product k from country i to destination n in year t. The key parameter of interest is the estimated fixed effect $\hat{\eta}_{i,k,t}^{(-j)}$, which captures the idiosyncratic supply-side variation specific to exporter i for product k, estimated using the sample of all destination countries except j.

This leave-one-out sampling is essential for the exclusion restriction: by omitting the direct trade flows to country j, we ensure that the instrument $\hat{\eta}_{i,k,t}^{(-j)}$ is not contaminated by the idiosyncratic demand shocks or preferences of the importer j currently under analysis. One potential concern is that $\hat{\eta}_{i,k,t}^{(-j)}$ may still be correlated with global demand cycles specific to product k. We address this through a two-layered defense. First, the importer-year fixed effects ($FE_{n,t}$) in the shifter estimation absorb destination-specific macroeconomic shocks, ensuring that η is not driven by the aggregate business cycles of other importers. Second, and more importantly, our main 2SLS specification includes high-dimensional Industry-Year fixed effects. This controls for broader global demand shifts at the sectoral level, allowing us to identify price and quantity movements driven by exporter-specific supply capacity that deviates from global industry trends.[3]

[3] In future iterations of this paper, we plan to further strengthen this identification by implementing a region-level leave-one-out approach following Amiti et al. (2019) and exploring alternative specifications that include product-year fixed effects in the shifter estimation stage to fully isolate exporter-specific idiosyncratic shocks from global product cycles.

2.5 Empirical Specification

To identify how a product's structural importance in the global production network modulates the propagation of supply shocks, we employ a two-stage least squares (IV-2SLS) framework. This approach allows us to estimate the causal impact of exporter-side supply shocks on both import prices and quantities, and specifically, how these effects vary with the centrality of the traded product.

In the first stage, we examine the pass-through of supply shocks to import prices by estimating the following equation:

$$\Delta \ln p_{ijkt} = \beta_1 \hat{\eta}_{ikt}^{(-j)} + \beta_2 (\hat{\eta}_{ikt}^{(-j)} \times C_{it-1}) + FE_{it} + FE_{jt} + FE_{st} + \epsilon_{ijkt} \tag{6}$$

where p_{ijkt} is the unit price of product k from exporter i to importer j at time t. The term $\hat{\eta}_{ikt}^{(-j)}$ represents our leave-out supply shifter, and C_{it-1} is the structural centrality of product k in country i. We include exporter-year (FE_{it}) and importer-year (FE_{jt}) fixed effects to control for time-varying macroeconomic conditions in each market, and industry-year (FE_{st}) fixed effects (where s corresponds to the BEA-USIO industry classification) to account for global industry-specific shocks. The coefficient β_2 captures the "buffer effect." If high-centrality goods serve as systemic infrastructure for the global economy, their prices may exhibit greater stickiness—potentially due to the high social cost of price volatility or long-term contractual rigidities—leading to a negative β_2.

In the second stage, we estimate the quantity response to these predicted price changes:

$$\Delta \ln q_{ijkt} = \sigma_1 \Delta \ln \hat{p}_{ijkt} + \sigma_2 (\Delta \ln \hat{p}_{ijkt} \times C_{it-1}) + FE_{it} + FE_{jt} + FE_{st} + \nu_{ijkt} \tag{7}$$

where q_{ijkt} is the imported quantity and $\Delta \ln \hat{p}_{ijkt}$ is the predicted price change from the first stage. The coefficient σ_1 corresponds to the standard Armington elasticity. Our focus is σ_2, the "network amplification effect," which tests whether the structural importance of a node triggers a chain of substitution across downstream industries, resulting in an amplified aggregate quantity adjustment.

Our empirical framework provides two distinct contributions to the literature. First, by utilizing structural centrality derived from our high-granularity hybrid ICIO table, we explore the structural heterogeneity of shock propagation—specifically the tension between the "buffer effect" and the "choke point" hypothesis. High granularity is essential for this purpose, as standard ICIO tables are too coarse to accurately identify the systemic hubs that define the topology of GVCs.

Second, our identification strategy utilizes a supply-side shifter that leverages the rich variation in bilateral trade microdata. Traditional methods for estimating Armington elasticities—including the GMM approach of Feenstra (1994), the frameworks reviewed by Burstein and Gopinath (2014), or tariff-based instruments—often rely on selective policy changes or shocks limited to specific products. In contrast, our approach provides a universal measurement of

supply shocks across all traded categories, ensuring comprehensive coverage of the production network.

3 Results

3.1 Structural Properties and Shadow Hubs

Before presenting our main estimation results, we provide descriptive evidence on the structural properties of the global production network. Our primary measure of interest is the structural centrality, calculated as the eigenvector of the global Leontief inverse under unit final demand ($F = 1$). This measure isolates the "pervasiveness" of a product—the degree to which it serves as a critical, common input across the global economy—independent of the scale of final consumption.

The skewed distribution of centrality. The descriptive statistics of structural centrality reveal a highly skewed, power-law-like distribution. As summarized in the statistics, the median centrality score is 0.62, while the mean is 0.94. Crucially, the maximum value reaches 79.28 (for the iron and steel sector in China), which is nearly two orders of magnitude higher than the median. This "fat-tail" property suggests that the GVC is anchored by a small number of ultra-central nodes that function as the systemic infrastructure of global production.

Decoupling from trade volume. Table 1 presents the top 30 sector-country pairs ranked by structural centrality for the year 2019, immediately preceding the global pandemic. The ranking is dominated by upstream intermediate sectors such as iron and steel mills, nonferrous metal smelting, and electronic components. A striking feature of this ranking is the frequent decoupling between structural importance and trade volume. We refer to these systemically essential but transactionally modest nodes as "shadow hubs."

For instance, China's nonferrous metal smelting sector ranks 4th in global structural centrality, yet it ranks only 334th in its global trade rank by export value. Conversely, high-volume consumer goods often exhibit relatively lower structural centrality despite their prominence in trade value. This discrepancy highlights that transaction scale is an insufficient proxy for a sector's role as a structural anchor in the global supply chain.

To formally examine this relationship, Figure 1 presents a log-log scatter plot of trade volume against structural centrality. While a baseline regression reveals a positive correlation, the significant vertical dispersion around the trend line confirms that structural centrality captures a distinct dimension of the GVC topology that is not subsumed by mere transaction scale. The observations located in the lower-right region of the plot represent these bottleneck sectors: products that are essential to a vast array of downstream processes despite their relatively modest trade values in the global market.

Table 1. Top 30 Sectors by Structural Centrality (2019)

Rank	Country	Sector Name (NAICS-based)	Centrality	Trade Rank
1	CHN	Iron and steel mills and ferroalloy manufacturing	81.73	31
2	CHN	Fabric mills	64.64	18
3	CHN	Broadcast and wireless communications equipment	56.71	2
4	CHN	Nonferrous metal (ex. aluminum) smelting and refining	41.46	334
5	CHN	Semiconductor and related device manufacturing	41.29	6
6	RUS	Oil and gas extraction	38.83	4
7	SAU	Oil and gas extraction	32.68	3
8	CHN	Other electronic component manufacturing	31.88	17
9	RUS	Nonferrous metal (ex. aluminum) smelting and refining	31.51	125
10	RUS	Iron and steel mills and ferroalloy manufacturing	30.06	110
11	JPN	Iron and steel mills and ferroalloy manufacturing	27.21	68
12	CHN	Other basic organic chemical manufacturing	27.09	23
13	DEU	Iron and steel mills and ferroalloy manufacturing	26.98	85
14	ITA	Iron and steel mills and ferroalloy manufacturing	25.13	167
15	CHN	Leather and allied product manufacturing	24.86	12
16	CHN	Printed circuit assembly (electronic assembly) mfg.	23.10	101
17	RUS	Petroleum refineries	22.97	15
18	CHN	Motor and generator manufacturing	22.89	155
19	SGP	Semiconductor and related device manufacturing	22.33	30
20	AUS	Iron, gold, silver, and other metal ore mining	21.46	14
21	KOR	Semiconductor and related device manufacturing	20.91	7
22	CHN	Plastics material and resin manufacturing	20.83	222
23	DEU	Nonferrous metal (ex. aluminum) smelting and refining	19.96	221
24	CHN	Aluminum product mfg. from purchased aluminum	19.85	243
25	TUR	Iron and steel mills and ferroalloy manufacturing	19.61	238
26	JPN	Nonferrous metal (ex. aluminum) smelting and refining	18.40	251
27	KOR	Iron and steel mills and ferroalloy manufacturing	17.45	102
28	IND	Iron and steel mills and ferroalloy manufacturing	17.19	275
29	CHN	Synthetic rubber and artificial synthetic fibers mfg.	17.05	236
30	USA	Petroleum refineries	16.57	10

Notes: This table reports the top 30 sectors ranked by structural centrality for the year 2019. Centrality is the structural centrality score calculated under unit final demand ($F = 1$) based on our high-granularity hybrid ICIO table. Trade Rank refers to the global rank of the exporter-sector pair in terms of total export value in 2019.

The identification of these shadow hubs provides the empirical foundation for our subsequent analysis. Given their role as pervasive common inputs, the social and economic costs of price volatility for these central goods are exceptionally high. This structural positioning creates strong incentives for firms to maintain price stability through long-term contractual rigidities or strategic pricing, providing the logical basis for the "structural buffer effect" tested in Section 4.2.

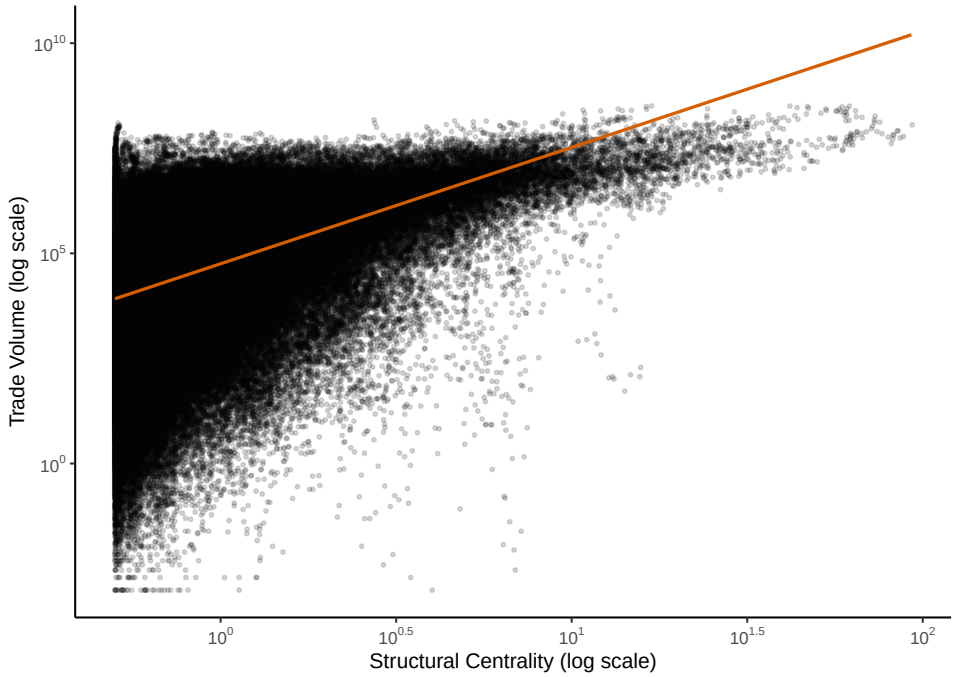


Figure 1. Structural Centrality vs. Trade Volume (1995–2023)
Notes: The figure plots structural centrality against trade volume for all sector-country pairs pooled over the period 1995–2023 ($N = 469,439$).The regression line indicates a positive correlation with a slope of 2.768 and $R^2 = 0.191$.

3.2 Centrality and the Structural Buffer Effect

The core of our empirical analysis follows a three-part logical structure: establishing the validity of identification, estimating primary trade parameters, and exploring structural shifts during the COVID-19 pandemic.

Price pass-through and the structural buffer effect. Table 2 reports the first-stage estimates of the pass-through of supply shocks to import prices. The baseline result in Column (1) shows that a negative supply shock leads to a statistically significant increase in import prices, confirming that our supply-side shifters effectively capture cost-push pressures. [4]

A key finding is the striking asymmetry revealed in Column (2). Specifically, while a negative supply shock carries a coefficient of −0.0096, the marginal effect of a positive shock is significantly offset by the interaction term (+0.0066), resulting in a much smaller net coefficient of −0.0030 for supply gluts. This implies that the upward price pressure from supply shortages is more than three times as strong as the downward pressure from gluts, a result consistent with the narrative of downward price rigidity in intermediate goods markets.

This stark asymmetry provides the empirical justification for the subsample analysis in Columns (3) and (4), where we separately examine how network topology modulates directional

[4]While the pass-through coefficient of −0.0071 is statistically robust, its modest magnitude reflects the idiosyncratic nature of the leave-one-out shifter, which isolates pure supply-side variation independent of aggregate demand trends.

shocks. While the interaction with centrality is negligible for positive shocks (Column 3), it is positive and highly significant (+0.0044) for negative shocks (Column 4). The positive sign of this interaction is economically critical: since the supply shock η is negative, a positive coefficient on the interaction term effectively acts as a brake on the price increase. This suggests that for more central products, the cost-push pressure is endogenously dampened, confirming that the buffer effect is a mechanism specifically triggered during supply disruptions.

Quantitatively, for a product with structural centrality one standard deviation above the mean—representing a systemic hub that serves as a significantly more pervasive common input compared to the average product—the price hike triggered by a negative supply shock (−0.0114) is mitigated by approximately 40% relative to the baseline. This indicates that high-centrality nodes effectively function as systemic infrastructure. A potential explanation for this finding is that because these goods are critical to a vast array of downstream industries, the social and economic costs of price volatility could be exceptionally high. Such systemic importance may incentivize firms to maintain price stability through long-term contractual rigidities or other structural stabilizers, effectively dampening the pass-through of idiosyncratic shocks.

Table 2. Price pass-through and the structural buffer effect

Dep. variable:	Change in import price ($\Delta \ln p$)			
	Baseline (1)	Asymmetry (2)	Positive (3)	Negative (4)
Supply shock (η)	−0.0071***	−0.0096***	−0.0044**	−0.0114***
	(0.0016)	(0.0017)	(0.0018)	(0.0016)
$\eta\times$ Pos. shock flag		0.0066***		
		(0.0012)		
$\eta\times$ Centrality			0.0002	0.0044***
			(0.0008)	(0.0007)
Fixed effects:				
Importer × Year	Yes	Yes	Yes	Yes
Exporter × Year	Yes	Yes	Yes	Yes
Industry × Year	Yes	Yes	Yes	Yes
Observations	124,917,547	124,917,547	49,491,426	75,426,121
R-squared	0.00931	0.00931	0.00941	0.00954

Notes: The table reports estimated coefficients from the first-stage price pass-through regressions for the full sample (1995–2023). Column (1) presents the baseline pass-through. Column (2) examines the asymmetry between positive and negative shocks. Columns (3) and (4) test the structural buffer effect by interacting the supply shock with topological centrality. Standard errors in parentheses are clustered at the exporter and industry levels. ***, **, and * denote significance at the 1, 5, and 10 percent levels.

Armington elasticity and the network amplification effect. Table 3 presents the second-stage results for quantity responses. Our baseline IV-2SLS estimate for the Armington elasticity is

approximately −4.766 (Column 1), which aligns with standard estimates found in the international trade literature (e.g., Feenstra, 1994; Burstein and Gopinath, 2014; Fontagné, Guimbard, and Orefice, 2022). The contrast with the OLS estimate of −0.6595 in Column (5) is stark. This significant discrepancy underscores that unobserved demand shocks frequently mask the true underlying price sensitivity of trade flows; specifically, the OLS coefficient suffers from attenuation bias because positive demand shocks drive simultaneous increases in both prices and quantities, creating a positive correlation that offsets the negative price elasticity and biases the coefficient toward zero.

Column (2) examines potential asymmetry in quantity responses. Unlike the price pass-through results, the interaction term for positive shocks is statistically insignificant, suggesting that the baseline demand elasticity remains relatively symmetric across directional shocks. However, a comparison of the subsample results in Columns (3) and (4) reveals a nuanced role for network topology. While the base elasticity for positive shocks is somewhat lower in absolute terms (−3.587) than for negative shocks (−4.729), the network amplification effect is nearly twice as large in the negative subsample (−0.4075) compared to the positive one (−0.2418).

This finding indicates that structural centrality plays a more decisive role in modulating quantity adjustments during supply disruptions. The intuition behind this amplification may lie in the "chain of substitution" enabled by the production network. When the price of a structurally central input rises due to a supply shortage, it potentially triggers a simultaneous search for substitutes across numerous downstream industries. While this mechanism operates for both types of shocks, the search intensity and resulting quantity adjustment are particularly pronounced for negative shocks: while a supply glut offers a cost-saving opportunity, a supply shortage represents a systemic risk of production halts, compelling firms to activate alternative supply pathways more aggressively. This aggregate adjustment, compounded across the network topology, results in a significantly more sensitive quantity response for central goods than for peripheral ones, especially when supply is constrained.

3.3 Topological Neutralization during COVID-19

Table 4 investigates the structural stability of shock propagation by comparing the pre-pandemic baseline (1995–2019) with the pandemic recovery period (2021–2023). To isolate the impact of supply-chain disruptions, we focus on the subsample of negative supply shocks ($\eta < 0$), excluding the transition year of 2020. The results reveal a striking asymmetry: the structural mechanisms governing price formation remained persistent, whereas the network-driven heterogeneity in quantity adjustments was effectively neutralized.

In the first stage (Columns 1 and 2), we find that the structural buffer effect is a robust feature of the GVC. The interaction between supply shocks and centrality remains positive and significant in both periods, with coefficients of +0.0044 and +0.0032, respectively. This persistence suggests that the capacity of central nodes to dampen cost-push pressures is an

Table 3. Demand elasticity and the network amplification effect

Dep. variable:	Change in import quantity ($\Delta \ln q$)				
	IV-2SLS				OLS
	Baseline	Asymmetry	Positive	Negative	Baseline
Price change ($\Delta \ln \hat{p}$)	-4.766^{***}	-5.126^{***}	-3.587^{***}	-4.729^{***}	-0.6595^{***}
	(0.6938)	(0.7319)	(1.033)	(0.5316)	(0.0136)
$\Delta \ln \hat{p} \times$ Pos. shock		-0.1146			
		(0.3035)			
$\Delta \ln \hat{p} \times$ Centrality			-0.2418^{**}	-0.4075^{*}	
			(0.0930)	(0.2311)	
Fixed effects:					
Importer × Year	Yes	Yes	Yes	Yes	Yes
Exporter × Year	Yes	Yes	Yes	Yes	Yes
Industry × Year	Yes	Yes	Yes	Yes	Yes
Observations	124,917,547	124,917,547	49,491,426	75,426,121	124,917,547
1st-stage F ($\Delta \ln \hat{p}$)	1,477.3	805.8	39.6	668.0	–
1st-stage F (Interact.)	–	18,582.5	915.7	3,813.5	–

Notes: Results for the second-stage demand elasticity regressions (1995–2023). Columns (1) to (4) instrument import prices with supply shocks (η) and their interactions. Column (5) provides OLS estimates for comparison. First-stage F-statistics indicate strong identification across all specifications. Standard errors in parentheses are clustered at the exporter and industry levels. ***, **, and * denote significance at the 1, 5, and 10 percent levels.

inherent structural property of the production network, likely anchored by long-term relational contracts that prioritize price stability for systemic inputs.

In contrast, the second-stage results exhibit a profound regime shift. In the pre-pandemic period, the interaction term is −0.3702, consistent with the long-run evidence that GVC centrality typically amplifies quantity adjustments. However, during the COVID-19 recovery, this interaction effect drops to a negligible −0.0426.

We interpret this as a topological neutralization of quantity adjustments. Notably, while the network-driven amplification disappeared, the baseline price elasticity remained statistically stable (shifting from −4.533 to −4.851). This indicates that while importers' fundamental price sensitivity was preserved, their ability to exploit alternative supply paths—the theoretical "chain of substitution" inherent in high-centrality nodes—was paralyzed by pervasive physical bottlenecks. In this environment, the network's topological advantages vanished, forcing all sectors to follow a uniform adjustment path regardless of their position in the production network.

Table 4. Regime shift in GVC dynamics: Pre-COVID vs. COVID recovery

Stage:	Stage 1: Pass-through		Stage 2: Elasticity	
Period:	Pre-COVID	COVID	Pre-COVID	COVID
	(1)	(2)	(3)	(4)
Supply shock (η) / Price change ($\Delta \ln \hat{p}$)	−0.0118***	−0.0115***		
	(0.0018)	(0.0030)		
η or $\Delta \ln \hat{p}$× Centrality	0.0044***	0.0032*	−0.3702	−0.0426
	(0.0008)	(0.0014)	(0.2011)	(0.2508)
Price change ($\Delta \ln \hat{p}$)			−4.533***	−4.851***
			(0.5225)	(1.118)
Fixed effects:				
Importer × Year	Yes	Yes	Yes	Yes
Exporter × Year	Yes	Yes	Yes	Yes
Industry × Year	Yes	Yes	Yes	Yes
Observations	61,624,211	9,779,195	61,624,211	9,779,195
1st-stage F ($\Delta \ln \hat{p}$)	–	–	580.3	78.4
1st-stage F (Interact.)	–	–	2,985.1	1,124.9

Notes: This table compares the GVC dynamics between the pre-pandemic (1995–2019) and COVID recovery (2021–2023) periods. The transition year of 2020 is excluded. All columns are restricted to the subsample of negative supply shocks ($\eta < 0$). Columns (1) and (2) report OLS estimates for the first-stage price pass-through. Columns (3) and (4) report IV-2SLS estimates for the second-stage elasticity, where prices and their interactions are instrumented by exporter-side supply shocks (η) and their corresponding interactions. First-stage F-statistics are reported for both the price change and its interaction with centrality. Standard errors in parentheses are clustered at the exporter and industry levels. ***, **, and * denote significance at the 1, 5, and 10 percent levels.

4 Conclusion

This paper has investigated the propagation of supply shocks and their impact on inflationary pressures through Global Value Chains (GVCs). By utilizing highly granular trade microdata and a high-granularity hybrid ICIO table, we provide new evidence that the structural topology of the production network plays a decisive role in modulating both price pass-through and quantity adjustments.

Our findings document two primary empirical regularities that characterize the modern GVC. First, we identify a persistent "structural buffer effect," where products with high structural centrality—which we term "shadow hubs"—exhibit significantly dampened price increases in response to negative supply shocks. These central nodes act as structural anchors for global price stability across different economic regimes, likely governed by long-term relational contracts that prioritize price stability for systemic inputs.

Second, we find a profound regime shift in quantity adjustment dynamics during the COVID-19 recovery period. While network centrality typically amplifies quantity adjustments in the long run through a "chain of substitution"—a process where the high density of connections around central nodes allows downstream sectors to access alternative supply pathways—this mechanism was effectively paralyzed during the crisis. This "topological neutralization" occurred even as baseline price elasticities remained stable, indicating that while buyers' fundamental price sensitivity was preserved, their ability to activate these alternative pathways was restricted by pervasive physical bottlenecks.

These results offer significant implications for monetary policy and the monitoring of global supply-side inflation. By identifying systemic choke points that transaction-scale metrics often fail to capture, our framework provides a robust indicator for assessing the origins of inflationary pressures. For policymakers, these findings suggest a potential decoupling of price signals from physical shortages within the network's core. The persistent price-buffering role of shadow hubs implies that inflationary pressures may remain latent in official price indices while physical disruptions accumulate. This signal attenuation, combined with the temporary loss of the network's substitution capacity, creates a hidden vulnerability where localized shocks can transform into systemic supply-chain failures that are difficult for traditional demand-side policies to address.

The empirical regularities established in this paper provide a foundation for several promising avenues of future research. A natural next step is to develop a theoretical framework that formalizes the state-dependent nature of price buffering and the topological neutralization of quantity adjustments. Such a model would ideally incorporate micro-foundations of relational contracting and endogenous capacity constraints within a production network. Understanding the interaction between these structural frictions and network topology is essential for addressing the signal-extraction problem and designing optimal stabilization policies in an increasingly interconnected and supply-constrained global economy.

References

Acemoglu, D., Carvalho, V. M., Ozdaglar, A., & Tahbaz-Salehi, A. (2012). "The Network Origins of Aggregate Fluctuations." *Econometrica*, 80(5), 1977–2016.

Amiti, M., Itskhoki, O., & Konings, J. (2019). "International Shocks, Variable Markups, and Domestic Prices." *The Review of Economic Studies*, 86(6), 2356–2402.

Antràs, P., Chor, D., Fally, T., & Hillberry, R. (2012). "Measuring the Upstreamness of Production and Trade Flows." *American Economic Review*, 102(3), 412–416.

Autor, D. H., Dorn, D., & Hanson, G. H. (2013). "The China Syndrome: Local Labor Market Effects of Import Competition in the United States." *American Economic Review*, 103(6), 2121–2168.

Baqaee, D. R., & Farhi, E. (2019). "The Macroeconomic Impact of Microeconomic Shocks: Beyond Hulten's Theorem." *Econometrica*, 87(4), 1155–1203.

Baqaee, D. R., & Farhi, E. (2022). "Supply and Demand in Disaggregated Keynesian Economies with an Application to the COVID-19 Crisis." *American Economic Review*, 112(5), 1397–1436.

Barrot, J.-N., & Sauvagnat, J. (2016). "Input Specificity and the Propagation of Idiosyncratic Shocks in Production Networks." *The Quarterly Journal of Economics*, 131(3), 1543–1592.

Bhattacharyya, A., Kutlu, L., & Sickles, R. C. (2019). "Shadow Prices." In *The Palgrave Handbook of Economic Performance Analysis*, 511–540. Palgrave Macmillan, Cham.

Burstein, A., & Gopinath, G. (2014). "International Prices and Exchange Rates." In *Handbook of International Economics*, edited by G. Gopinath, E. Helpman, and K. Rogoff, Vol. 4, 391–451. Amsterdam: Elsevier.

Carvalho, V. M. (2014). "From Micro to Macro: The Case of Production Networks." *Journal of Economic Perspectives*, 28(4), 23–48.

Carvalho, V. M., Nirei, M., Saito, Y. U., & Tahbaz-Salehi, A. (2021). "Supply Chain Disruptions: Evidence from the Great East Japan Earthquake." *The Quarterly Journal of Economics*, 136(2), 1255–1321.

di Giovanni, J., Kalemli-Özcan, Ş., Silva, A., & Yildirim, M. A. (2022). "Global Supply Chain Disruptions and Inflation during the Pandemic." *NBER Working Paper* No. 30240.

Feenstra, R. C. (1994). "New Product Varieties and the Measurement of International Prices." *American Economic Review*, 84(1), 157–177.

Ferrari, A. (2025). "Inventories, Demand Shocks Propagation, and Amplification in Supply Chains." *Working Paper*.

Fontagné, L., Guimbard, H., & Orefice, G. (2022). "Tariff-based product-level trade elasticities." *Journal of International Economics*, 137, 103593.

Gabaix, X. (2011). "The Granular Origins of Aggregate Fluctuations." *Econometrica*, 79(3), 733–772.

Hummels, D., Jørgensen, R., Munch, J., & Xiang, C. (2014). "The Wage Effects of Offshoring: Evidence from Danish Matched Worker-Firm Data." *American Economic Review*, 104(6), 1597–1629.

Jones, C. I. (2011). "Intermediate Goods and Weak Links in the Theory of Economic Development." *American Economic Journal: Macroeconomics*, 3(2), 1–28.

Katz, L. (1953). "A new status index derived from sociometric analysis." *Psychometrika*, 18(1), 39–43.

Macchiavello, R. (2022). "Relational Contracts and Development." *Annual Review of Economics*, 14, 337–362.

Miller, R. E., & Blair, P. D. (2022). *Input-Output Analysis: Foundations and Extensions*. 3rn Edition. Cambridge University Press.

Nunn, N. (2007). "Relationship-specificity, incomplete contracts, and the pattern of trade." *The Quarterly Journal of Economics*, 122(2), 569–600.

Pasten, E., Schoenle, R., & Weber, M. (2020). "The Propagation of Monetary Policy Shocks in a Heterogeneous Production Economy." *Journal of Monetary Economics*, 116, 1–22.

Santacreu, A. M., & LaBelle, J. (2022). "Supply Chain Disruptions and Inflation during the COVID-19 Pandemic." *Federal Reserve Bank of St. Louis Review*, 104(3), 211–232.

Weitzman, M. L. (1974). "Prices vs. Quantities." *The Review of Economic Studies*, 41(4), 477–491.